Blue Flashes as Counterparts to Narrow Bipolar Events: the Optical Signal of Shallow In-Cloud Discharges

Dongshuai Li[1], Alejandro Luque[1], F. J. Gordillo-Vázquez[1], Feifan Liu[2], Gaopeng Lu[2],

Torsten Neubert[3], Olivier Chanrion[3], Baoyou Zhu[2], Nikolai Østgaard[4], Víctor Reglero[5]

[1]Instituto de Astrofísica de Andalucía (IAA), CSIC, Granada, Spain.

[2]CAS Key Laboratory of Geospace Environment, School of Earth and Space Sciences, University of Science and

Technology of China, Hefei, China

[3]National Space Institute, Technical University of Denmark (DTU Space), Kongens Lyngby, Denmark.

[4]Birkeland Centre for Space Science, Department of Physics and Technology, University of Bergen, Bergen, Norway

[5]Image Processing Laboratory, University of Valencia, Valencia, Spain

Key Points:

- Blue luminous events are only detected in the 337 nm photometer and its filtered camera, with no signal in 777.4 nm optical band.
- Blue luminous events are found to be associated with the negative narrow bipolar events inside the thunderstorm.
- Narrow bipolar events have streamer-like structures and the numbers of steamer branches for them were evaluated.

Corresponding author: Dongshuai Li, Alejandro Luque, `dsl@iaa.es`, `aluque@iaa.es`. Instituto de Astrofísica de Andalucía (IAA), CSIC,Granada, Spain.

Abstract

On August 7, 2019, eight Blue LUminous Events (BLUEs) above a thunderstorm over South China were detected by the Modular Multispectral Imaging Array (MMIA) of the Atmosphere-Space Interactions Monitor (ASIM), the Vaisala GLD360 global lightning network and the very low frequency (VLF)/low frequency (LF) sensor at Guangzhou. All events coincided with negative-polarity Narrow Bipolar Event (NBE) radio detections. The 337-nm photometer detected the strongest optical signal; in some events there was a weak signal in 180-230 nm but no signal was detected in 777.4 nm. The light-curves are consistent with sources spanning a few kilometers below the cloud tops and allow us to estimate the source extension and optical energy in the 337-nm band, corresponding to the energy emitted by fast breakdown involving around 10^9 streamer initiation events.

Plain Language Summary

Installed on the International Space Station (ISS), the Atmosphere-Space Interactions Monitor (ASIM) is designed to observe Earth thunderstorms from space. Often it detects bursts of blue light emerging from active thunderclouds. These detections have been previously linked to radio signals named Narrow Bipolar Events (NBEs) that are routinely detected during a thunderstorm. Here we analyze the blue flashes from a storm that profusely produced negative-polarity NBEs. The optical signal can be understood as being produced by extended events close to the cloud top and we show that it is consistent with the barely understood electrical discharge process called fast breakdown that involves a huge number of thin, bright filaments called streamers.

1 Introduction

Blue LUminous Events (hereafter, BLUEs), such as blue jets and blue starters, are transient electrical phenomena that occur in active thunderstorms and are characterized by optical signals strongly dominated by the blue range of the spectrum and lasting from about one millisecond to hundreds of milliseconds. They were first reported by Wescott et al. (1995, 1996) in the framework of the Sprites 1994 aircraft campaign. After these initial reports, BLUEs have been observed and investigated mainly from space-based platforms: for example, from black-and-white camera of the Space Shuttle (Boeck et al., 1998), from the limb-pointing Imager of Sprites/Upper Atmospheric Lightning (ISUAL) onboard FORMOSAT-2 (Kuo et al., 2005; Chou et al., 2011, 2018), from off-the-shelf cameras on the International Space Station (ISS) (Chanrion et al., 2017) and, most recently, from the Modular Multispectral Imaging Array (MMIA) of the Atmosphere-Space Interactions Monitor (ASIM) onboard the ISS since April 2, 2018 (Soler et al., 2020; Neubert et

al., 2021). BLUEs can also be observed from the ground, as reported by Edens (2011), but this is complicated due to Rayleigh scattering and extinction by intervening clouds.

As we define them here, BLUEs comprise several phenomena. Blue jets normally emerge out of the cloud top and reach altitudes about 40 km - 50 km at speeds of the order of 100 km/s (Wescott et al., 2001). Blue starters terminate at lower altitudes, typically around 18 km but sometimes up to 25 km and advance with velocities 10 km/s to 100 km/s (Wescott et al., 1996); they are often described as initial phases of blue jets (Pasko, 2008) and hence their name. Other types of BLUEs have also been reported, including small blue surface discharges (sometimes called *blue glimpses*) that appear to "dance" on the upper layer of the cloud at a rate of about 120 per minute (Chanrion et al., 2017) and the *gnomes* that emerge directly from the cloud top within $\sim$ 1 km, similar to blue starters, but with brighter and more uniform optical emission and much more compact shape (Lyons et al., 2003). *Giant jets*, which travel from cloud tops to the lower ionosphere, may also be classified as BLUEs although they involve measurable emissions in the 777.4-nm band (van der Velde et al., 2019).

Each of these types of phenomena exhibits a different morphology but they likely share common physical processes. The blue color indicates the presence of electron-impact excitation of molecular nitrogen (Pasko, 2008; Surkov & Hayakawa, 2020; F. Gordillo-Vázquez & Pérez-Invernón, 2021) and the weak or absent atomic oxygen line at 777.4 nm, indicates that air does not reach high temperatures, typically associated with lightning leaders at ground level. This points to streamer coronas being the key component of BLUEs, a conclusion supported by the close association between BLUEs and Narrow Bipolar Events (NBEs) (F. Liu et al., 2018; Soler et al., 2020), which are radio emissions also attributed to corona discharges in thunderclouds (Rison et al., 2016; Tilles et al., 2019; N. Liu et al., 2019). It is thus likely that both BLUEs and NBEs are electromagnetic manifestations of large streamer coronas (or *fast breakdown*, a term coined by Rison et al. (2016) that we also adopt here).

Some distinctive features of each type of BLUE arise from their extension and their location inside the thundercloud. For example, Soler et al. (2020) analyzed a set of 10 BLUEs associated with positive NBEs and at a considerable depth inside the cloud, presumably between the main negative and the upper positive charge region of the cloud. As these events are deeply buried in the cloud, the scattering by cloud droplets and ice crystals blurs their image as observed from above, resulting in a diffuse blob that can be identified with the blue glimpses reported by Chanrion et al. (2017).

Here we focus on events that are close to the cloud top, perhaps partially outside the cloud. This location suggest an origin between the upper negative region of the cloud and the positively charged screening layer, and this is supported by radio detections that associate these events with negative-polarity NBEs (Lyu et al., 2015; Wu et al., 2012; Smith et al., 1999). Because the emissions

come from close to the cloud top, optical radiation is less affected by scattering, leading to a more robust inference of source characteristics. This allows us to compare to radio observations of fast breakdown.

2 Instruments and Observations

The Modular Multispectral Imaging Array (MMIA) is a component of the Atmosphere-Space Interactions Monitor (ASIM), a mission launched on April 2, 2018 and installed on the International Space Station (Chanrion et al., 2019; Neubert et al., 2019). MMIA observes in ultraviolet and near-infrared wavelengths, points towards the nadir and contains three photometers and two cameras. The three photometers, with a temporal sampling rate of 100 kHz, include one in the UV band at 180 nm to 230 nm, and two others sensitive to the same wavelengths as two installed cameras: in the near-UV at the strongest spectral line of the nitrogen second positive system (337 nm) and at the strongest lightning emission line, OI (777.4 nm). The spatial resolution of the cameras is around 400 m × 400 m at the nadir point and their integration time is 83.3 ms.

On the evening of August 7 2019, above an intense localized thunderstorm over Southern China, there were eight blue luminous events (BLUEs) simultaneously detected by MMIA, the ground-based Vaisala GLD360 global lightning network and the ground-based very low frequency (VLF)/low frequency (LF) sensor at Guangzhou (see Table 1 for further details). All of them were detected by MMIA's photometer and camera filtered at 337 nm; some events had a detectable signal in the 180 nm to 230 nm photometer but there was no signal in the 777.4 nm photometer and camera at the 3σ confidence level. Depending on the event this implies that the 777.4-nm flux was at least between 50 and 300 times weaker than the 337-nm flux (see Figure S1 in supplemental material for more details). The rise times of the events in the 337 nm photometer are below 56 μs, with the shortest of them being unresolved by the 10 μs sampling time of the photometer. The peak brightness ranges from 20 to 140 μW/m^2, which is among the brightest signals detected by MMIA. The brightness and quick rise of the events indicate that they originate close to the cloud tops or perhaps slightly above them. Note however that below we show that most of the emissions were partially scattered by the cloud and that the photometer light curve is not indicative of the true source duration.

We sketch the context of the eight BLUEs in Figure 1 which, in panels (a) and (b), plots the intra-cloud (IC) and cloud-to-ground (CG) flashes and the eight BLUEs superimposed on the cloud top height (CTH) provided by the Fengyun-4A (FY-4A) satellite (Yang et al., 2017) for the time period from 13:04:00 to 13:07:00 UTC. During these three minutes, there were 522 lightning events with 240 CG and 282 IC flashes reported by GLD360 (see Figure 1). Two of the BLUE events (with ID 5 and 7) were missing from GLD360 so for all the BLUEs we use the location provided by the lightning location systems (LLSs) in Guangzhou province (Chen et al., 2012).

The absolute timing uncertainty of MMIA is on the order of tens of milliseconds but we can correct the MMIA times to sub-millisecond accuracy by comparing flash times provided by GLD360 to MMIA 777.4 nm-pulses. In our case we found that the systematic time shift with respect to the ground-based measurements experienced a time adjustment at around 13:06:07, the time corrections before and after the time adjustment are (-23.3 ± 0.3) ms and (-6.2 ± 0.5) ms, respectively (see Figure S2 in Supplemental material for further details). Note that the time shift -23.3 ms is similar to the estimations for other thunderstorms such as the -28.7 ms inferred by Soler et al. (2020) or the -16.37 ms from Neubert et al. (2021).

With this time correction we find that each of the eight BLUEs has a radio signal that, when back-propagated to the source, is within 0.7 ms of the optical peak. All VLF/LF waveforms of the BLUEs were unambiguously classified as negative NBEs (see Figure 2 for examples) measured by the vertical electric field antenna (frequency bandwidth 800 Hz to 400 kHz) located about 105 km away at Guangzhou station of Jianghuai Area Sferic Array (JASA) (Qin et al., 2015; F. Liu et al., 2018). The radio signals of the eight events, along with other positive NBEs at deeper locations in the same thunderstorm, are analyzed with more details in a complementary publication (F. Liu et al., 2021).

Figure 1 shows in panels (c) and (d) a composition of all camera images for the BLUE events (always from the 337 nm-filtered camera). To produce this picture we have added the projection of each of the eight MMIA images into the Earth surface according to coordinates introduced by the ASIM pipeline. The resulting locations differ noticeably from those provided by LLSs and the distribution is more spread out. We attribute this to uncertainties in the camera orientation. Note also that several of the images exhibit a sharp peak that appears to emerge from the middle of the diffuse blob: this is a blooming artifact of the CCD camera.

To understand better the relation between the BLUE emissions and their parent thunderstorm, we examined the progression of the cloud Top Blackbody Brightness temperature (TBB in K) provided by the Himawari-8 satellite (Bessho et al., 2016) with ten-minute resolution . Figure S3 in Supplemental material displays the TBB around the time of our detections. The BLUE events originated from the boundary of a rapidly-evolving thunderstorm cell. This suggests that rapid turbulent mixing of the screening layer plays a role in the inception of fast breakdown (Krehbiel et al., 2008; Lyons et al., 2003) or the occurrence of groups of localized NBEs is associated with dynamically intense convection (Bandara et al., 2021). Note that the altitudes provided by FY-4A that we use here are likely underestimates since negative NBEs are usually associated with deep convection and detected in overshooting cloud tops (F. Liu et al., 2018; Wu et al., 2013).

Table 1. The eight BLUEs simultaneously detected by MMIA, ground-based Vaisala GLD360 global lightning network and the ground-based VLF/LF sensor at Guangzhou. All the detection times have been corrected to the time with respect to the BLUEs source locations.

ID	Date (Year/Month/Day)	MMIA time UTC(Source)	MMIA corrected time UTC(Source)	GLD360 time UTC(Source)	VLF/LF time UTC(Source)	Rise Time [a] (µs)	Time duration [b] (µs)	Peak Brightness (µW/m²)
1	2019/08/07	13:05:56.9362	13:05:56.9595	13:05:56.9594	13:05:56.9594	31.17	371.36	20.11
2	2019/08/07	13:05:58.6317	13:05:58.6550	13:05:58.6549	13:05:58.6549	8.04	196.72	142.18
3	2019/08/07	13:06:01.7568	13:06:01.7801	13:06:01.7800	13:06:01.7799	56.30	758.77	40.61
4	2019/08/07	13:06:09.5668	13:06:09.5730	13:06:09.5722	13:06:09.5723	8.71	399.46	97.88
5	2019/08/07	13:06:16.6329	13:06:16.6391	-	13:06:16.6384	13.07	912.33	44.51
6	2019/08/07	13:06:20.9670	13:06:20.9732	13:06:20.9726	13:06:20.9726	14.08	486.78	120.30
7	2019/08/07	13:06:30.4934	13:06:30.4996	-	13:06:30.4993	13.07	334.22	46.48
8	2019/08/07	13:06:31.6557	13:06:31.6619	13:06:31.6616	13:06:31.6615	13.40	237.87	39.96

[a] Rise time is calculated using the linear interpolation by taking the time for the amplitude of a photometer signal to rise from 10% to 90%. Note that the sampling time is 10 µs so the rise is unresolved in several events.

[b] Time duration is calculated using the linear interpolation by the time interval for the amplitude of a photometer signal to rise from 10% and fall to 10%.
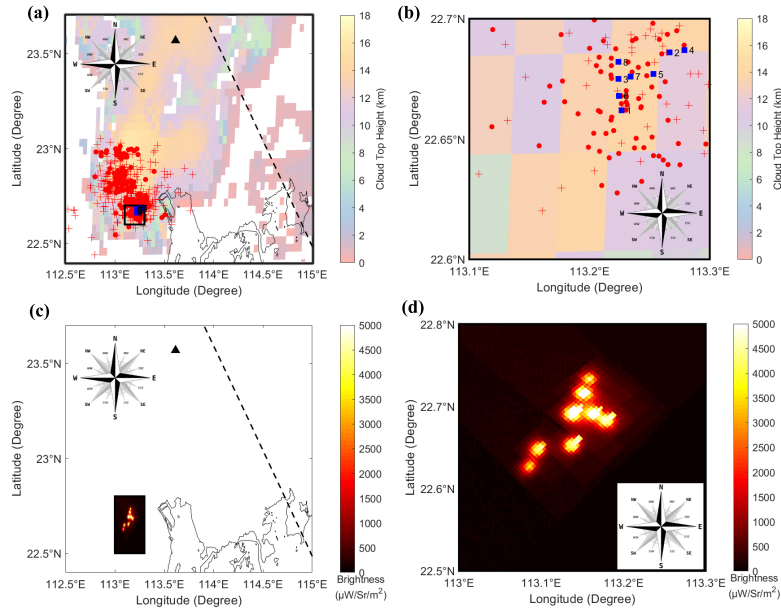

Figure 1. Distribution of the CG/IC lightning and eight BLUEs along with Cloud Top Height (CTH) at the time period from 13:04:00 to 13:07:00 UTC (a) and the zoom of its black rectangular region (b) (Red dots: CG lightning detected by GLD360, Red crosses: IC lightning detected by GLD360 and Blue squares: BLUEs detected by LLSs); eight BLUEs images detected in the 337 nm filtered camera of MMIA (c) and the zoom (d). The ground-based VLF/LF sensor at Guangzhou is shown as black triangle. The footprints of ASIM are shown in black dashed line.

3 Light-scattering model

To better understand the MMIA observations we compare them now to a simple model where the light source is a thin, straight, uniformly bright segment and the cloud is homogeneous with a planar upper boundary. We neglect the intrinsic duration of the source, assuming that all light is emitted instantaneously.

Because photons can be scattered many times before they exit the cloud, an impulsive optical flash results in a temporally stretched light curve. To understand this curve we start with the expression for a point-like source buried in the cloud. Using the diffusion approximation for the propagation of photons inside the cloud proposed by Koshak et al. (1994), Soler et al. (2020) gave an analytical expression for this curve, which was derived in more detail by Luque et al. (2020). Adopting the normalization and the notation of the later, the photon flux exiting the cloud top reads

$$\Gamma(t) = NF(t) = \frac{Ne^{-t/\tau_A - \tau_D/t}}{\pi^{1/2}\tau_D}\left(\frac{t}{\tau_D}\right)^{-3/2}, \tag{1}$$

where $F(t)$ is the flux per photon in the source, N is the total number of source photons, τ_A is the mean absorption time of the photons inside the cloud and $\tau_D = L^2/4D$ is, given a diffusion coefficient D, the characteristic time of diffusion for the distance L between the source and the cloud top. The derivation of these magnitudes from the microscopic properties of the cloud is given by Koshak et al. (1994) and reviewed by Luque et al. (2020). Equation (1) is valid for $t > 0$, where the time origin is the moment of light emission. For a distant observer, differences in light travel time from different points in the cloud are not significant so one can reinterpret the time in equation (1) with $t = 0$ being the arrival time of an unscattered photon.

To obtain the light curve for an extended source that spans altitudes from the cloud top to a maximum depth L_0 we integrate $(N/L_0)F(t)dL$ from 0 to L_0 (the factor N/L_0 is the linear density of source photons, assumed uniform). The result is

$$\Gamma_L(t) = N\left(\frac{D}{t}\right)^{1/2}\left(1 - e^{-\tau_D/t}\right)e^{-t/\tau_A}, \ \tau_D = L_0^2/4D. \tag{2}$$

Note that this expression disregards any part of the source above the cloud top. Some photons emitted outside the cloud propagate directly to the detector and others are back-scattered by the upper cloud surface after a small number of scattering events. These emissions have an effect only on a few data points in a photometer with a $10\,\mu s$ time resolution. We therefore do not account for these emissions which, although may be present, do not dominate the photometer light-curves.

For short times after the emission, equation (2) predicts a $\sim t^{-1/2}$ dependence for the flux that is cut off by either photon absorption with a time-scale τ_A or by the finite size of the source, with a time-scale τ_D (see Figure S4 in supplemental material). The cutoff from the mean absorption time is likely negligible: Luque et al. (2020) estimates $\tau_A \approx 2.3\,ms$ for clouds composed by water droplets

175 with an effective radius of 20 µm and a droplet density of 10^8 m^{-3} but this possibly overestimates the

176 absorption. The cloud tops are dominated by ice particles, which absorb radiation at 337 nm several

177 orders of magnitude less efficiently than water (Warren & Brandt, 2008). Besides, the available

178 estimates of the extinction coefficient (Peterson, 2020; Platt, 1997) also lead to absorption times

179 significantly longer than the duration of our events. Hence here we assume $\tau_A \gg \tau_D$.

180 As we show in Figure S4 in the supplemental material, most of the recorded BLUEs light-

181 curves have the shape predicted by equation (2). In the figure we plot a least-squares fit of the

182 observational data to the model with two parameters: an overall amplitude factor and the decay time

183 τ_D. To reduce the effect of the emissions from outside the cloud discussed above, we disregard the

184 data points at the peak of the light-curve. The good fit of most events indicate that indeed they

185 originate from sources that extend below the cloud top. Event 5 is the only one that does not show a

186 clear $t^{-1/2}$ decay, possibly because there was a gap between the source and the cloud top or because

187 light emissions were inhomogeneous or long-lasting. In events 1 and 7 there is weak secondary

188 activity 1 ms to 2 ms after the main peak that distorts the estimate of the cutoff time τ_D.

189 Leaving aside events where τ_D was estimated poorly, this cutoff time ranges between 0.5 ms

190 and 1.6 ms. The smallest diffusion coefficient proposed by Soler et al. (2020), $D = 3 \times 10^9$ m^{2}s^{-1}

191 yields a range of lengths for the optical sources of $L_0 = 2.4$ km to 4.4 km. However, the evaluated

192 results will be affected by the uncertainties that surround our modeling of the cloud composition.

193 Next we extend our model to include the propagation of the signal to the MMIA instruments,

194 accounting for Rayleigh scattering by the atmosphere and for the non-isotropic (approximately Lam-

195 bertian) emission pattern from the cloud tops. We use the radiative transfer Monte Carlo code Cloud-

196 Scat.jl (Luque et al., 2020) and run simulations of uniformly bright, straight vertical sources, with

197 the lengths L_0 derived above, in a homogeneous cloud that spans altitudes from 7 km to the cloud top

198 height derived by the Fengyun-4A (FY-4A) satellite (listed in Table 2). The scattering parameters in

199 the cloud are those for a density of 10^8 m^{-3} spherical ice particles with 20 µm radius. The relative

200 positions between the source and the observer reproduce the conditions of each of the eight BLUEs

201 in our dataset.

202 In Figure 2 we show the results of the Monte Carlo code comparing with 337-nm photometer

203 and camera observations for the event 2 and 8 (Additional comparisons can be found in Figure

204 S5-S12 in supplemental material). The photometer light curves calculated from CloudScat model

205 closely follow the analytical estimate of equation (2) and are a good fit to the observations. The

206 simulated camera images are also reasonably close to MMIA's records although they are slightly

207 more compact. This is a possible indication of a non-negligible source width on the order of the

208 camera resolution of about 400 m.

Table 2. Model-inferred properties of the eight BLUE events. We list the cloud top height measured by FY-4A at the event location, the best-fit cutoff time τ_D (see equation (2)), the resulting source length $L_0 = (4D\tau_D)^{1/2}$ with $D = 3 \times 10^9$ m^{2}s^{-1}, the total optical energy in the 337-nm band of the second positive system of nitrogen and an estimation of the number of streamer branching events in the fast breakdown processes that we assume that originated the events.

ID	Cloud top height (km)	Cutoff time (τ_D) (ms)	Source length (L_0) (km)	Optical energy at 337 nm (J)	Branching events
1	11.2	19.6[a]	-[a]	1.8×10^4	1.4×10^9
2	11.6	1.6	4.4	1.9×10^4	1.4×10^9
3	14.0	1.2	3.8	1.2×10^4	9.1×10^8
4	13.1	0.5	2.4	1.3×10^4	9.8×10^8
5	11.6	8.6[b]	-[b]	2.4×10^4	1.9×10^9
6	14.0	0.8	3.1	1.8×10^4	1.4×10^9
7	14.0	3.8[a]	-[a]	1.6×10^4	1.2×10^9
8	14.0	0.5	2.5	4.6×10^3	3.6×10^8

[a] In events 1 and 7 there is secondary activity that distorted the estimation of the cutoff time τ_D and the source length.

[b] Event 5 has a light-curve that cannot be explained by an impulsive, uniformly bright source.
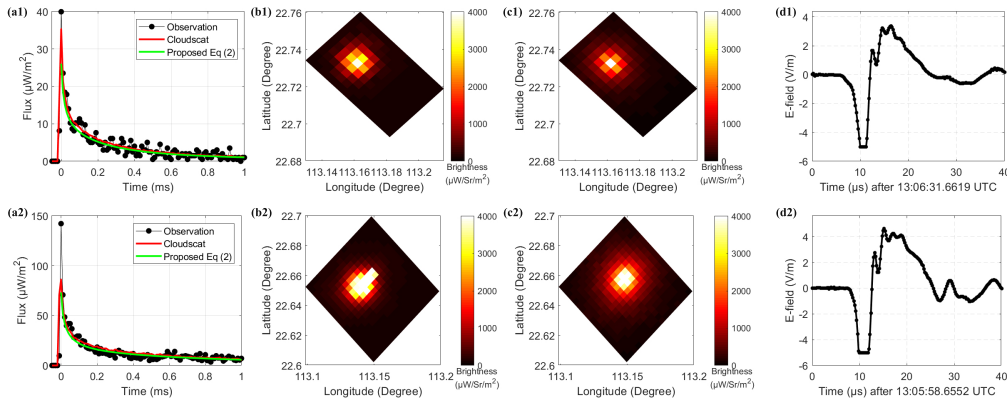
Figure 2. Comparing the modeling results against the observation of MMIA for event 8 (a1 - d1) and event 2 (a2 - d2). The 337 nm photometer signals (a1, a2): MMIA observation (black dotted line), modeling results by using CloudScat model (red line) and the proposed equation (2) (green line). The images measured by 337 nm filtered camera of MMIA (b1, b2). The simulated images obtained from CloudScat model (c1, c2). The waveforms of the NBEs detected from the ground-based VLF/LF sensor at Guangzhou (d1, d2).

In the results presented here we always consider that the top of the source coincides with the top of the cloud. As we discuss above, the effect of light emissions outside the cloud is too impulsive to

compare against the MMIA photometer and is possibly dominated by the intrinsic time-dependence of the source. We performed additional Monte Carlo simulations that confirm that the photometer light-curves are compatible with source tops within a few hundred meters of the cloud top, either above or below it. The VLF/LF waveforms of negative NBEs for event 2 and 8 are also shown in Figure 2.

The CloudScat.jl code outputs a photon flux at the observer's location in units of photons per unit time and unit surface that reach a detector for each photon in the source whereas the MMIA photometers are calibrated in terms of power per unit surface (irradiance). The conversion factor is the total energy of the event in the 337 band, $E = Nhc/\lambda$, where N is the total number of photons emitted by the source, h is the Planck's constant, c is the speed of light and $\lambda = 337$ nm. By comparing the results of our Monte Carlo code to the MMIA data we found the best-matching total energy of each event. Because the events that we analyze are close to the cloud tops and thus barely affected by in-cloud absorption, our estimates of E are weakly sensitive to our model assumptions and thus provide a reasonably precise picture of the actual source emission intensity of the BLUE events. The estimated energies are listed in Table 2.

N. Liu et al. (2019) analyzed radio spectra of NBEs and concluded that they can be understood as systems of 10^7 to 10^8 streamers. In that analysis the key feature of a streamer is a current moment that increases rapidly on a time scale of about one nanosecond, which is the timescale of streamer initiation in numerical simulations. Here we also consider that a single nanosecond event may produce more than one streamer, as is the case in a bifurcated tree. Denoting by b the mean number of streamers emerging from an event, we have $M = bK$, where M is the total number of streamers (unbifurcated branches) and K is the number of initiation events (most likely bifurcations from other streamers). Then the total streamer length contained in one fast breakdown process is ℓbK, where ℓ is the mean length between bifurcations (but see Nijdam et al. (2020) for a discussion of the difficulties involved in precisely defining this quantity). If a streamer emits η photons per unit length as it propagates, the total number of emitted photons is $N = \eta\ell bK$.

It follows from the scaling laws for streamers (Ebert et al., 2010) that η depends on air density only through collisional quenching of the radiative states of N_2 (the remaining factor is proportional to $\pi R^2 n_e$ where R is the streamer radius, which scales as the inverse of air density, and n_e is the electron density, which scales as the square of air density). The numerical simulations by Malagón-Romero & Luque (2019) predict a time-integrated photon yield of about 2×10^{18} m^{-3} in a streamer of radius $R \approx 2$ mm. From the spectra presented by F. J. Gordillo-Vázquez et al. (2012), we infer that about 30% of these emissions are inside the 5-nm window of the 337-nm MMIA photometer, yielding $\eta \approx (n_0/n) \times 2 \times 10^{12}$ m^{-1}, where n_0/n is the ratio of air density at atmospheric-pressure, n_0, to the density at the altitude of interest, n. Here we take $n_0/n \approx 6$ for an altitude of 14 km. Briels et al. (2008) observed a ratio of branching length to streamer radius of about 20, so a radius of 2 mm

at atmospheric pressure translates into $\ell \approx (n_0/n) \times 4\,\text{cm} = 24\,\text{cm}$. We take the branching number b to be 2, although there are evidences that it may possibly be larger (Heijmans et al., 2013, 2015).

The estimation of the number of streamer branches for all the BLUEs are listed in Table 2. Our results are 10-100 times above those derived from radio spectra by N. Liu et al. (2019). One possible reason for this disagreement is the uncertainties in our assumed parameters. For example, the estimated K is highly sensitive to the assumed streamer radius: had we chosen a radius of 5 mm at atmospheric pressure, the estimation of K would be reduced by about a factor 15. It is also possible that a large fraction of the optical signal in fast breakdown is emitted not close to streamer heads but from long-lived glows, as is the case in sprites (Luque et al., 2016; Pérez-Invernón et al., 2020).

4 Discussion and conclusions

The eight BLUE events that we analyze in this paper expand and complete the picture of fast breakdown as the source of both optical blue-dominated emissions and radio pulses detected as NBEs in the VLF/LF bands or high-amplitude noise in VHF. All events were strongly detected in the photometer and camera filtered at 337 nm; in some events there was a weak signal in 180-230 nm but with no signal in 777.4 nm photometer and camera.

As in previous studies (Wescott et al., 1995, 1996; Chanrion et al., 2017), the BLUEs appeared temporally isolated from either CG or IC flashes detected by the GLD360 network. However, all the BLUEs coincide with NBEs observed by the ground-based VLF/LF sensor at Guangzhou. This strengthens the connection between BLUEs and negative NBEs (Chou et al., 2018; F. Liu et al., 2018) and further supports that NBEs originate from non-thermal, streamer processes (Rison et al., 2016; Lyu et al., 2019; Tilles et al., 2019; Soler et al., 2020).

The rise times of the blue events in the 337 nm photometer are between $10\,\mu\text{s}$ to $70\,\mu\text{s}$ with peak irradiance varying from $20\,\mu\text{Wm}^{-2}$ to $140\,\mu\text{Wm}^{-2}$. The brightness and short rise times suggest a source close or even slightly above the cloud tops and this is supported by our modeling results based either on the diffusion approximation by Koshak et al. (1994) or on a Monte Carlo radiative transfer code (Luque et al., 2020). Since all events are identified as negative NBEs, this is consistent with previous studies that localize the initiation of most of negative NBEs between the upper positive charge region and the screening charge region of the thunderstorm (Smith et al., 1999; Wu et al., 2012; Lyu et al., 2015). The variation in the rise times between different events may be due to differences in the intrinsic time dependence of the optical sources but this is equally well explained by a finite distance to the cloud top or from non-uniformities of the optical sources below the cloud.

Our estimates of the total optical energy within the 337-nm band provide a new constraint for models of fast breakdown. The present understanding of these events is still limited and it is difficult

to translate this energy into microscopical properties of fast breakdown. However our results confirm that fast breakdown involves more than 10^7 streamers, as inferred by N. Liu et al. (2019) and further analyzed by Cooray et al. (2020).

Future investigations should address the underlying physics of fast breakdown and its global significance, including its relation to lightning initiation. Data from the ASIM mission will likely play a decisive role in this research.

Acknowledgments

References

Bandara, S., Marshall, T., Karunarathne, S., & Stolzenburg, M. (2021). Groups of narrow bipolar events within thunderstorms. *Atmospheric Research*, *252*, 105450. doi: https://doi.org/10.1016/j.atmosres.2021.105450

Bessho, K., Date, K., Hayashi, M., Ikeda, A., Imai, T., Inoue, H., . . . others (2016). An introduction to Himawari-8/9—Japan's new-generation geostationary meteorological satellites. *Journal of the Meteorological Society of Japan. Ser. II*, *94*(2), 151–183.

Boeck, W. L., Vaughan, O. H., Blakeslee, R., Vonnegut, B., & Brook, M. (1998). The role of the space shuttle videotapes in the discovery of sprites, jets and elves. *Journal of Atmospheric and Solar-Terrestrial Physics*, *60*(7), 669 - 677. doi: https://doi.org/10.1016/S1364-6826(98)00025

-X

Briels, T. M. P., van Veldhuizen, E. M., & Ebert, U. (2008, nov). Positive streamers in air and nitrogen of varying density: experiments on similarity laws. *Journal of Physics D: Applied Physics*, *41*(23), 234008. doi: 10.1088/0022-3727/41/23/234008

Chanrion, O., Neubert, T., Mogensen, A., Yair, Y., Stendel, M., Singh, R., & Siingh, D. (2017). Profuse activity of blue electrical discharges at the tops of thunderstorms. *Geophysical Research Letters*, *44*(1), 496-503. doi: https://doi.org/10.1002/2016GL071311

Chanrion, O., Neubert, T., Rasmussen, I. L., Stoltze, C., Tcherniak, D., Jessen, N. C., ... others (2019). The modular multispectral imaging array (MMIA) of the ASIM payload on the international space station. *Space Science Reviews*, *215*(4), 1–25.

Chen, L., Zhang, Y., Lu, W., Zheng, D., Zhang, Y., Chen, S., & Huang, Z. (2012). Performance evaluation for a lightning location system based on observations of artificially triggered lightning and natural lightning flashes. *Journal of Atmospheric and Oceanic Technology*, *29*(12), 1835–1844.

Chou, J. K., Hsu, R.-R., Su, H.-T., Chen, A. B.-C., Kuo, C.-L., Huang, S.-M., ... Wu, Y.-J. (2018). ISUAL-observed blue luminous events: The associated sferics. *Journal of Geophysical Research: Space Physics*, *123*(4), 3063-3077. doi: https://doi.org/10.1002/2017JA024793

Chou, J. K., Tsai, L. Y., Kuo, C. L., Lee, Y. J., Chen, C. M., Chen, A. B., ... Lee, L. C. (2011). Optical emissions and behaviors of the blue starters, blue jets, and gigantic jets observed in the taiwan transient luminous event ground campaign. *Journal of Geophysical Research: Space Physics*, *116*(A7).

Cooray, V., Cooray, G., Rubinstein, M., & Rachidi, F. (2020). Modeling compact intracloud discharge (CID) as a streamer burst. *Atmosphere*, *11*(5). doi: 10.3390/atmos11050549

Ebert, U., Nijdam, S., Li, C., Luque, A., Briels, T., & van Veldhuizen, E. (2010). Review of recent results on streamer discharges and discussion of their relevance for sprites and lightning. *Journal of Geophysical Research: Space Physics*, *115*(A7). doi: https://doi.org/10.1029/2009JA014867

Edens, H. E. (2011). Photographic and lightning mapping observations of a blue starter over a new mexico thunderstorm. *Geophysical Research Letters*, *38*(17). doi: https://doi.org/10.1029/2011GL048543

Gordillo-Vázquez, F., & Pérez-Invernón, F. (2021). A review of the impact of transient luminous events on the atmospheric chemistry: Past, present, and future. *Atmospheric Research*, *252*, 105432. doi: https://doi.org/10.1016/j.atmosres.2020.105432

Gordillo-Vázquez, F. J., Luque, A., & Simek, M. (2012). Near infrared and ultraviolet spectra of TLEs. *Journal of Geophysical Research: Space Physics*, *117*(A5). doi: https://doi.org/10.1029/2012JA017516

Heijmans, L. C. J., Clevis, T., Nijdam, S., Van Veldhuizen, E., & Ebert, U. (2015). Streamer

knotwilg branching: sudden transition in morphology of positive streamers in high-purity nitrogen. *Journal of Physics D: Applied Physics*, *48*(35), 355202.

Heijmans, L. C. J., Nijdam, S., van Veldhuizen, E. M., & Ebert, U. (2013, jul). Streamers in air splitting into three branches. *EPL (Europhysics Letters)*, *103*(2), 25002. doi: 10.1209/0295-5075/103/25002

Koshak, W. J., Solakiewicz, R. J., Phanord, D. D., & Blakeslee, R. J. (1994). Diffusion model for lightning radiative transfer. *Journal of Geophysical Research: Atmospheres*, *99*(D7), 14361-14371. doi: https://doi.org/10.1029/94JD00022

Krehbiel, P. R., Riousset, J. A., Pasko, V. P., Thomas, R. J., Rison, W., Stanley, M. A., & Edens, H. E. (2008). Upward electrical discharges from thunderstorms. *Nature Geoscience*, *1*(4), 233–237.

Kuo, C.-L., Hsu, R. R., Chen, A. B., Su, H. T., Lee, L. C., Mende, S. B., . . . Takahashi, Y. (2005). Electric fields and electron energies inferred from the ISUAL recorded sprites. *Geophysical Research Letters*, *32*(19). doi: https://doi.org/10.1029/2005GL023389

Liu, F., Lu, G., Neubert, T., Lei, J., Chanrion, O., Østgaard, N., . . . Zhu, B. (2021). Optical emissions associated with narrow bipolar events in radio signals from thunderstorms. *Submitted to Nature communications*.

Liu, F., Zhu, B., Lu, G., Qin, Z., Lei, J., Peng, K.-M., . . . others (2018). Observations of blue discharges associated with negative narrow bipolar events in active deep convection. *Geophysical Research Letters*, *45*(6), 2842–2851.

Liu, N., Dwyer, J. R., Tilles, J. N., Stanley, M. A., Krehbiel, P. R., Rison, W., . . . Wilson, J. G. (2019). Understanding the radio spectrum of thunderstorm narrow bipolar events. *Journal of Geophysical Research: Atmospheres*, *124*(17-18), 10134-10153. doi: https://doi.org/10.1029/2019JD030439

Luque, A., Gordillo-Vázquez, F. J., Li, D., Malagón-Romero, A., Pérez-Invernón, F. J., Schmalzried, A., . . . Østgaard, N. (2020). Modeling lightning observations from space-based platforms (Cloudscat.jl 1.0). *Geoscientific Model Development*, *13*(11), 5549–5566. doi: 10.5194/gmd-13-5549-2020

Luque, A., Stenbaek-Nielsen, H. C., McHarg, M. G., & Haaland, R. K. (2016). Sprite beads and glows arising from the attachment instability in streamer channels. *Journal of Geophysical Research: Space Physics*, *121*(3), 2431-2449. doi: https://doi.org/10.1002/2015JA022234

Lyons, W. A., Nelson, T. E., Armstrong, R. A., Pasko, V. P., & Stanley, M. A. (2003). Upward electrical discharges from thunderstorm tops. *Bulletin of the American Meteorological Society*, *84*(4), 445–454.

Lyu, F., Cummer, S. A., & McTague, L. (2015). Insights into high peak current in-cloud lightning events during thunderstorms. *Geophysical Research Letters*, *42*(16), 6836-6843. doi: https://

doi.org/10.1002/2015GL065047

Lyu, F., Cummer, S. A., Qin, Z., & Chen, M. (2019). Lightning initiation processes imaged with very high frequency broadband interferometry. *Journal of Geophysical Research: Atmospheres*, *124*(6), 2994-3004. doi: https://doi.org/10.1029/2018JD029817

Malagón-Romero, A., & Luque, A. (2019). Spontaneous emergence of space stems ahead of negative leaders in lightning and long sparks. *Geophysical Research Letters*, *46*(7), 4029-4038. doi: https://doi.org/10.1029/2019GL082063

Neubert, T., Chanrion, O., Heumesser, M., Dimitriadou, K., Husbjerg, L., Rasmussen, I. L., . . . Reglero, V. (2021). Observation of the onset of a blue jet into the stratosphere. *Nature*, *589*(7842), 371–375.

Neubert, T., Østgaard, N., Reglero, V., Blanc, E., Chanrion, O., Oxborrow, C. A., . . . Bhanderi, D. D. (2019). The ASIM mission on the international space station. *Space Science Reviews*, *215*(2), 1–17.

Nijdam, S., Teunissen, J., & Ebert, U. (2020, Nov). The physics of streamer discharge phenomena. *Plasma Sources Science and Technology*, *29*(10), 103001. doi: 10.1088/1361-6595/abaa05

Pasko, V. P. (2008, nov). Blue jets and gigantic jets: transient luminous events between thunderstorm tops and the lower ionosphere. *Plasma Physics and Controlled Fusion*, *50*(12), 124050. doi: 10.1088/0741-3335/50/12/124050

Peterson, M. (2020). Modeling the transmission of optical lightning signals through complex 3-D cloud scenes. *Journal of Geophysical Research: Atmospheres*, *125*(23), e2020JD033231. (e2020JD033231 2020JD033231) doi: https://doi.org/10.1029/2020JD033231

Platt, C. M. R. (1997). A parameterization of the visible extinction coefficient of ice clouds in terms of the ice/water content. *Journal of Atmospheric Sciences*, *54*(16), 2083–2098.

Pérez-Invernón, F. J., Malagón-Romero, A., Gordillo-Vázquez, F. J., & Luque, A. (2020). The contribution of sprite streamers to the chemical composition of the mesosphere-lower thermosphere. *Geophysical Research Letters*, *47*(14), e2020GL088578. (e2020GL088578 10.1029/2020GL088578) doi: https://doi.org/10.1029/2020GL088578

Qin, Z., ZHU, B., MA, M., MA, D., et al. (2015). Using time domain waveforms of return strokes to retrieve the daytime fluctuation of ionospheric D layer. *Chinese Science Bulletin*, *60*(7), 654–663.

Rison, W., Krehbiel, P. R., Stock, M. G., Edens, H. E., Shao, X.-M., Thomas, R. J., . . . Zhang, Y. (2016). Observations of narrow bipolar events reveal how lightning is initiated in thunderstorms. *Nature communications*, *7*(1), 1-12.

Smith, D. A., Shao, X. M., Holden, D. N., Rhodes, C. T., Brook, M., Krehbiel, P. R., . . . Thomas, R. J. (1999). A distinct class of isolated intracloud lightning discharges and their associated radio emissions. *Journal of Geophysical Research: Atmospheres*, *104*(D4), 4189-4212. doi: https://doi.org/10.1029/1998JD200045

Soler, S., Pérez-Invernón, F. J., Gordillo-Vázquez, F. J., Luque, A., Li, D., Malagón-Romero, A., ... Østgaard, N. (2020). Blue optical observations of narrow bipolar events by ASIM suggest corona streamer activity in thunderstorms. *Journal of Geophysical Research: Atmospheres*, *125*(16), e2020JD032708. (e2020JD032708 10.1029/2020JD032708) doi: https://doi.org/10.1029/2020JD032708

Surkov, V. V., & Hayakawa, M. (2020). Progress in the study of transient luminous and atmospheric events: A review. *Surveys in Geophysics*, *41*, 1101–1142.

Tilles, J. N., Liu, N., Stanley, M. A., Krehbiel, P. R., Rison, W., Stock, M. G., ... Wilson, J. (2019). Fast negative breakdown in thunderstorms. *Nature communications*, *10*(1), 1–12.

van der Velde, O. A., Montanyà, J., López, J. A., & Cummer, S. A. (2019). Gigantic jet discharges evolve stepwise through the middle atmosphere. *Nature communications*, *10*(1), 1–10.

Warren, S. G., & Brandt, R. E. (2008). Optical constants of ice from the ultraviolet to the microwave: A revised compilation. *Journal of Geophysical Research: Atmospheres*, *113*(D14). doi: https://doi.org/10.1029/2007JD009744

Wescott, E. M., Sentman, D., Osborne, D., Hampton, D., & Heavner, M. (1995). Preliminary results from the Sprites94 aircraft campaign: 2. blue jets. *Geophysical Research Letters*, *22*(10), 1209-1212. doi: https://doi.org/10.1029/95GL00582

Wescott, E. M., Sentman, D. D., Heavner, M. J., Hampton, D. L., Osborne, D. L., & Vaughan Jr., O. H. (1996). Blue starters brief upward discharges from an intense arkansas thunderstorm. *Geophysical Research Letters*, *23*(16), 2153-2156. doi: https://doi.org/10.1029/96GL01969

Wescott, E. M., Sentman, D. D., Stenbaek-Nielsen, H. C., Huet, P., Heavner, M. J., & Moudry, D. R. (2001). New evidence for the brightness and ionization of blue starters and blue jets. *Journal of Geophysical Research: Space Physics*, *106*(A10), 21549-21554. doi: https://doi.org/10.1029/2000JA000429

Wu, T., Dong, W., Zhang, Y., Funaki, T., Yoshida, S., Morimoto, T., ... Kawasaki, Z. (2012). Discharge height of lightning narrow bipolar events. *Journal of Geophysical Research: Atmospheres*, *117*(D5). doi: https://doi.org/10.1029/2011JD017054

Wu, T., Takayanagi, Y., Yoshida, S., Funaki, T., Ushio, T., & Kawasaki, Z. (2013). Spatial relationship between lightning narrow bipolar events and parent thunderstorms as revealed by phased array radar. *Geophysical Research Letters*, *40*(3), 618-623. doi: https://doi.org/10.1002/grl.50112

Yang, J., Zhang, Z., Wei, C., Lu, F., & Guo, Q. (2017). Introducing the new generation of chinese geostationary weather satellites, fengyun-4. *Bulletin of the American Meteorological Society*, *98*(8), 1637–1658.